Journal of Cluster Science (2024) 35:999–1005
https://doi.org/10.1007/s10876-023-02526-4

ORIGINAL PAPER

Magnetic Nanoparticles Encapsulated Zeolitic Imidazolate Frameworks: A New Delivery System for Crocin

Hani Nasser Abdelhamid[1,2] · Dina H. Kassem[3] · Rania M. Hathout[4]

Received: 17 September 2023 / Accepted: 10 November 2023 / Published online: 16 December 2023

Abstract

The synthesis of magnetic nanoparticles enclosed in zeolitic imidazolate frameworks (MNPs@ZIF-8) was successful carried out at ambient temperature and atmospheric pressure. The synthesis procedure was selected because it is uncomplicated and does not call for the use of any sophisticated pieces of apparatus throughout its execution. The Fourier transform infrared (FT-IR), X-ray diffraction (XRD), and transmission electron microscopy (TEM) images were investigated to characterize the materials. The analysis of the data allowed MNPs@ZIF-8 to evolve into a highly crystalline phase with particles ranging in size from 50 to 100 nanometers. This was made feasible by the fact that the phase could be created. It was explored whether or not MNPs@ZIF-8 was effective as a nanocarrier for the delivery of natural medicines like crocin. It was demonstrated to be very biocompatible and had an IC_{50} value of > 1000 µg/mL, which is the concentration at which half of the maximum inhibitory effect is produced. The IC_{50} value for crocin-loaded MNPs-ZIF-8 was 419 ± 0 µg/mL, which was roughly half of the IC_{50} value for pure crocin, which was 716 ± 160 µg/mL.

Keywords Crocin · Drug delivery · Natural anticancer · MOFs · ZIF-8 · Magnetic nanoparticles

Introduction

Natural drugs are currently thought of as advanced medicine offering high potency and low side effects. Carotenoid drugs such as Crocin are promising as an anticancer drug [1–5], a neural protective agent [6, 7], a pain killer [8], a hypolipidemic drug [9], an antidepressant [10], and an immunomodulator for COVID-19 treatment [11]. Crocin is the ester of saccharide gentiobiose and crocetin. It is a diester molecule composed of two units of gentiobiose and dicarboxylic groups of crocetin. It is a color pigment of natural flowers such as saffron that is extracted from the flower of *Crocus sativus*. It exhibits antioxidant activity via ROS (Reactive Oxygen Species) suppression of nuclear factor erythroid-derived 2 like 2 (denoted as Nrf2) and HO-1 [8, 12]. It also suppresses antioxidant enzymes, such as catalase and superoxide dismutase [13–15]. It can inhibit pancreatic lipase [9] and mitogen-activated protein kinase (MAPK). Crocin suppresses also the secretion of several biomolecules such as tumor necrosis factor (TNF-α), interleukin (IL-6, IL-10, IL-17, and IL-1β), and interferon-gamma (IFN-γ) [5, 8, 11]. The biological activity of crocin is considered interesting and further exploitation of its anti-cancer activity is important [8, 16]. Nanocarriers for drug delivery may advance the biomedical applications of crocin [17, 18].

Metal-organic frameworks (MOFs) improved several applications including drug delivery [19–23], catalysis [24, 25], and biomedical applications [26]. They offered several advantages such as high surface area enabling high drug loading [27]. The porosity of MOFs provides protection and maneuvering of the drug. Among several MOF materials, zeolitic imidazolate frameworks (ZIF-8) are highly reported and recommended as a carrier aiming for drug delivery

✉ Hani Nasser Abdelhamid
hany.abdelhamid@aun.edu.eg

✉ Rania M. Hathout
r_hathout@yahoo.com; rania.hathout@pharma.asu.edu.eg

[1] Department of Chemistry, Faculty of Science, Assiut University, Assiut, Egypt

[2] Nanotechnology Research Centre (NTRC), The British University in Egypt (BUE), El-Sherouk City, Suez Desert Road, Cairo 11837, Egypt

[3] Department of Biochemistry, Faculty of Pharmacy, Ain Shams University, Cairo 11566, Egypt

[4] Department of Pharmaceutics and Industrial Pharmacy, Faculty of Pharmacy, Ain Shams University, Cairo 11566, Egypt

[28–35]. ZIF-8 is highly biocompatible, can be used for the delivery of several drugs, and is relatively cheap. However, most of the reported ZIF materials are microporous and lack multifunctionality. ZIF8-based composites may enable high drug delivery and dual functionality. They can advance the applications of natural drugs.

Herein, a magnetic nanoparticle (MNPs i.e., Fe_3O_4) encapsulated ZIF-8 (MNPs@ZIF-8) was synthesized using a one-pot method to improve the delivery of crocin, taking into consideration the factors that were discussed before. ZIF material was used as a carrier for crocin, in cancer cell lines derived from the Michigan Cancer Foundation-7 (MCF-7). As a result, in the work that is being discussed here, a simple stirring process in a single pot procedure was chosen as the method for the synthesis of MNPs@ZIF-8 at room temperature. As a result, an easy way to produce these magnetic nanoparticles encapsulated MOFs was developed to obtain a drug delivery system for anti-cancer medicines such as crocin and other compounds with a comparable structure.

Experimental

Materials and Methods

2-methyl imidazole (Hmim, 99%, M.Wt. 82 g $mole^{-1}$), $Zn(NO_3)_2{\cdot}6H_2O$ (M.Wt. 297.49 g $mole^{-1}$, 98%), $Fe(NO_3)_3{\cdot}9H_2O$ (M.Wt. 404 g $mole^{-1}$, 98%), $FeSO_4{\cdot}7H_2O$ (278.01 g $mole^{-1}$, 98%), Crocin (M.Wt. = 977 g/mol), phosphate-buffered saline (PBS, 0.01M), and cellulose membrane (M.Wt cut-off 14000 Da) were obtained from Sigma–Aldrich (Germany).

Synthesis of MNPs and MNPs@ZIF-8

The method of co-precipitation was utilized in the synthesis of MNPs and MNPs@ZIF-8 [36]. In a volume of 25 milliliters of deionized water, solutions of ferrous and ferric salts were made by dissolving0.63 g and 1.73 g, respectively. The salts were co-precipitated in one hour using a solution of NH_4OH (25 mL, 30%), which was heated to 90 °C. MNPs made of iron oxide (Fe_3O_4) were isolated with the assistance of an external magnet. An aliquot of 0.2 g of the dried MNPs was put into a solution containing 0.67 mmol of $Zn(NO_3)_2$ solution. After that, a volume equal to 2 mL of the NaOH solution (0.01 mM) was added to the solution that had been created previously. At the end, 20 mL of Hmim containing 8 mmol was added. Before extracting the components with the assistance of an external magnet, the reaction solution was agitated at room temperature for a period of thirty minutes. Overnight, the materials were dried at 85 °C.

Preparation of Crocin-Loaded MNPs@ZIF-8

The adsorption post-loading approach was used to load crocin onto the synthetic MNPs@ZIF-8 [37]. In a nutshell, 20 mg of crocin was added to 10 mL of the MNPs@ZIF-8 suspension while it was being stirred at 600 revolutions per minute and heated to 25 °C. The material was cleaned up by dialyzing the crocin-loaded MNPs@ZIF-8 against one liter of PBS with a pH of 7.4 while it was heated to 25 °C [38]. The cleaned-up formulation was put to use in the following set of experiments. The percentage of drug loading efficiency was determined by measuring the amount of drug present in the dialyzed solution spectrophotometrically at 441 nm and then subtracting this amount from the total amount of drug that was initially added. This allowed for the calculation of the loading efficiency. Figure S1 and Table S1 both display the Crocin calibration curve in their respective formats.

The Release of Crocin: In-vitro Study

The release of free crocin from the crocin-loaded MNPs@ZIF-8 was recorded. 2 mL of each material containing 4 mg of crocin was added to a dialysis membrane bag. The membranes were soaked in 100 mL PBS (pH of 7.4) at 37 °C. At different times of 1, 2, 3, 4, 6, and 8 hours, 2 mL of the solution was collected for measuring via a spectrophotometer at a λ_{max} of 441 nm. The experiments were recorded in triplicates.

Culture and Maintenance of MCF-7 Breast Cancer Cell Lines

MCF-7 cells were cultured on RPMI-1640 medium supplemented with 10% fetal bovine serum, L-Glutamine (2 mM), penicillin (100 U/mL), streptomycin (100 µg/mL), and Amphotericin B (0.25 µg/mL, *Gibco, USA*). The cells were maintained at 37 °C in a humidified atmosphere with 5% CO_2 media that was changed every other day, and the cells were subcultured twice a week. For subculturing, Trypsin-EDTA 0.05% (*Lonza, Switzerland*) was used.

Cytotoxicity Evaluation Using Viability Assay

MCF-7 cells were prepared with a density of $1{\times}10^4$ cells for each well of a 96-well tissue culture plate. 200 µL of the culture medium was added to each well before incubation [24 h at 37 °C, a humidified atmosphere (5% CO_2)]. The culture medium was decanted and the cells were washed with sterile PBS. 200 µL of cell medium containing crocin aqueous solution or crocin-loaded MNPs@ZIF-8, or plain (unloaded)

MNPs@ZIF-8 were added at different concentrations following the same procedures. Control of the untreated cells maintained in a complete culture medium in the absence of any treatment was also done. The cells' viability after treatment was evaluated by MTT [3-(4,5-dimethylthiazol-2-yl)-2,5-diphenyltetrazolium bromide] method. Briefly, the media with various treatments was removed from all wells, and the cells were gently washed twice with PBS. Afterward, 150 µL of freshly prepared complete RPMI 1640 medium supplemented with MTT (0.5 mg/mL) was added to each well including the untreated control cells. Initially, a stock solution of MTT was freshly prepared with a concentration of 5 mg/mL in PBS. The media with MTT was discarded completely and 100 µL DMSO/well was added to dissolve the formed formazan crystals. Next, incubation was done for a total of 10 min at room temperature and then mixed thoroughly using a micro-plate shaker for 3 min. The optical density (OD) was recorded at a wavelength of 600 nm using a Chromate micro-plate reader (*Awareness Technologies, USA*). The cells' viability was calculated using the following equation [39, 40]:

$$\text{Cell viability} = \left[\left(\frac{OD_t}{OD_c}\right)\right] \times 100\%$$

where OD_t and OD_c are the mean optical density of wells treated and untreated cells, respectively. The relation between the percentage of viable cells and various drug/formulation concentrations was plotted to illustrate the concentration-dependent cell viability of the three groups; (1) crocin aqueous solution, (2) crocin-loaded MNPs@ZIF-8, and (3) plain MNPs@ZIF-8. The data analysis such as 50% inhibitory concentration (IC_{50}) was determined using Graph Pad Prism software (San Diego, CA. USA) [41–43]. The statistical analysis was also performed using the same software via the ANOVA method, $p < 0.05$.

Characterization Experiments

Using X-ray diffraction (a PANanalyticalX'Pert PRO diffractometer equipped with Cu Kα1 radiation), we were able to verify the crystallinity of the materials, as well as their phase identification and purity. Using transmission electron microscopy (TEM; JEOL, TEM-2100, Japan), we were able to determine the shape as well as the particle size of MNPs@ZIF-8. Using a Nicolet spectrophotometer model 6700, we were able to record the FT-IR spectra of both ZIF-8 and MNPs@ZIF-8.

Results and Discussion

Characterization and Drug Loading

Figure 1 shows the synthesis procedure of MNPs@ZIF-8 and crocin loading for drug delivery. The synthesis steps involved mixing ZIF-8 precursors i.e. Zn^{2+} ions and Hmim linker to Fe_3O_4 MNPs (Fig. 1). The one-pot synthesis procedure was adopted at room temperature using only stirring. Both components i.e. MNPs and ZIF-8 can be effective sites for drug adsorption. Thus, the composite can act as an effective carrier for drugs or potential therapeutic molecules such as crocin. The chemical structure of the drug shows several functional groups that reinforce the obtained materials i.e., MNPs@ZIF-8 was characterized using XRD (Fig. 2a), FT-IR (Fig. 2b), and TEM images (Fig. 3).

The phase purity was confirmed using XRD (Fig. 2a). The XRD patterns for simulated data and synthesized material are almost identical indicating the successful synthesis of the pure ZIF-8 phase (Fig. 2a). The XRD of ZIF-8 showed peaks at Bragg angles (2θ) of 7.4°, 10.5°, 12.8°, 14.8°, 16.5°, 18.1°, 22.2°, 24.6°, 26.8°, and 29.7°, corresponding to Miller indexes for planes of (011), (002), (112), (022), (013), (222), (114), (233), (134), and (044), respectively. There was no diffraction pattern for the magnetic nanoparticles due to the low loading of MNPs. The connectivity within the materials was evaluated using FT-IR (Fig. 2b). The obtained bands at a wavenumber of 1670 cm^{-1} and 1570 cm^{-1} are assigned to the stretching modes of C=C and C=N, respectively (Fig. 2b). The bands at 1137 cm^{-1}, 997 cm^{-1}, and 748 cm^{-1} refer to aromatic C–N stretching mode, C–N bending, and C–H bending, respectively. The band at 677 cm^{-1} is due to the out-of-plane bending of the imidazole ring of the linker i.e., Hmim. The characteristic peak of Zn–N stretching can be observed at 421 cm^{-1}(Fig. 2b). The magnetic nanoparticle shows a characterized peak at 542 cm^{-1} corresponding to Fe–O (Fig. 2b). XRD and FT-IR data confirm the synthesis of ZIF-8 and their composite with MNPs i.e. MNPs@ZIF-8.

The morphology and particle size were characterized using TEM images (Fig. 3). TEM image of ZIF-8 displayed aspherical crystals with particle sizes of 50–100 nm with an average particle size of 70.5 nm (Fig. 3a–b). The crystals showed mesopores inside the particle. On the other side, the TEM image for MNPs@ZIF-8 displayed the same crystal morphology of ZIF-8 crystals with dark particles belonging to the MNPs (Fig. 3b). MNPs displayed aspherical particles with an a particle size of 2–20 nm with an average particle size of 9.3 nm (Fig. 3b).

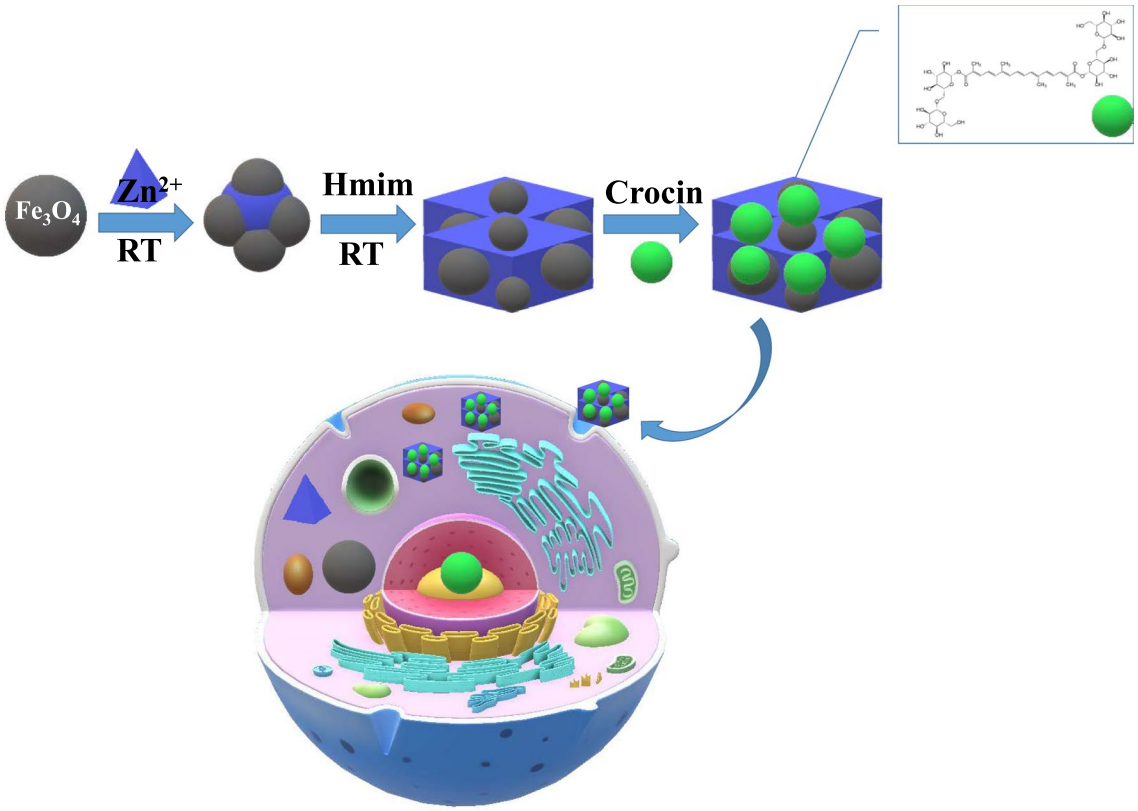

Fig. 1 Synthesis of MNPs@ZIF-8 and their application for crocin drug delivery. (RT stands for room temperature)

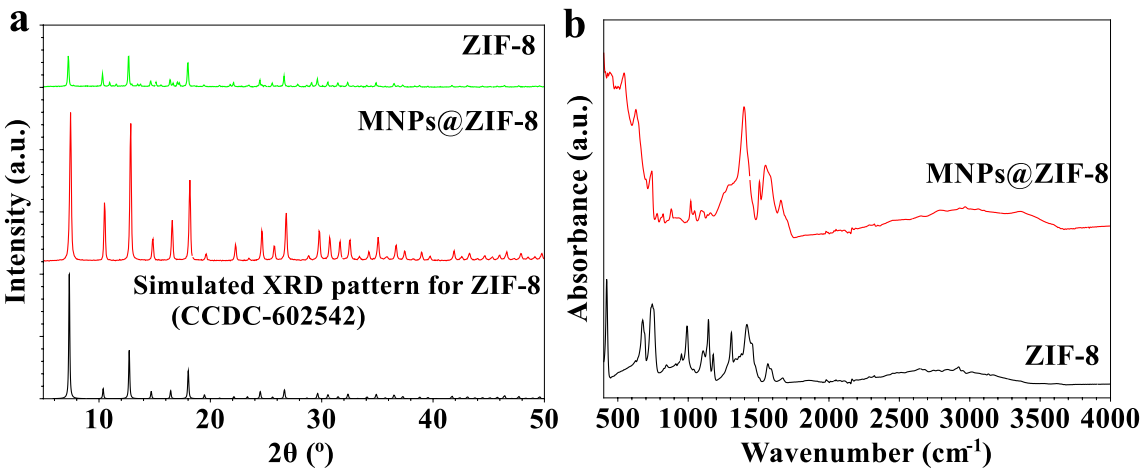

Fig. 2 Materials characterization using **a** XRD and **b** FT-IR

Crocin Loading and Delivery

Crocin was efficiently loaded on the MNPs@ZIF-8 scoring a value of 99.5 % ± 0.1. This should be attributed to the physical adsorption of the drug on the high surface area produced by MNPs@ZIF-8.

Figure 4 shows the release profile of crocin from the prepared MNPs@ZIF-8 as compared to its counterpart release from the aqueous solution. The release from the loaded MNPs@ZIF-8 lacked the burst initial effect that was notable and expected from the aqueous solution (90% of the total drug was released in the first hour) due to its

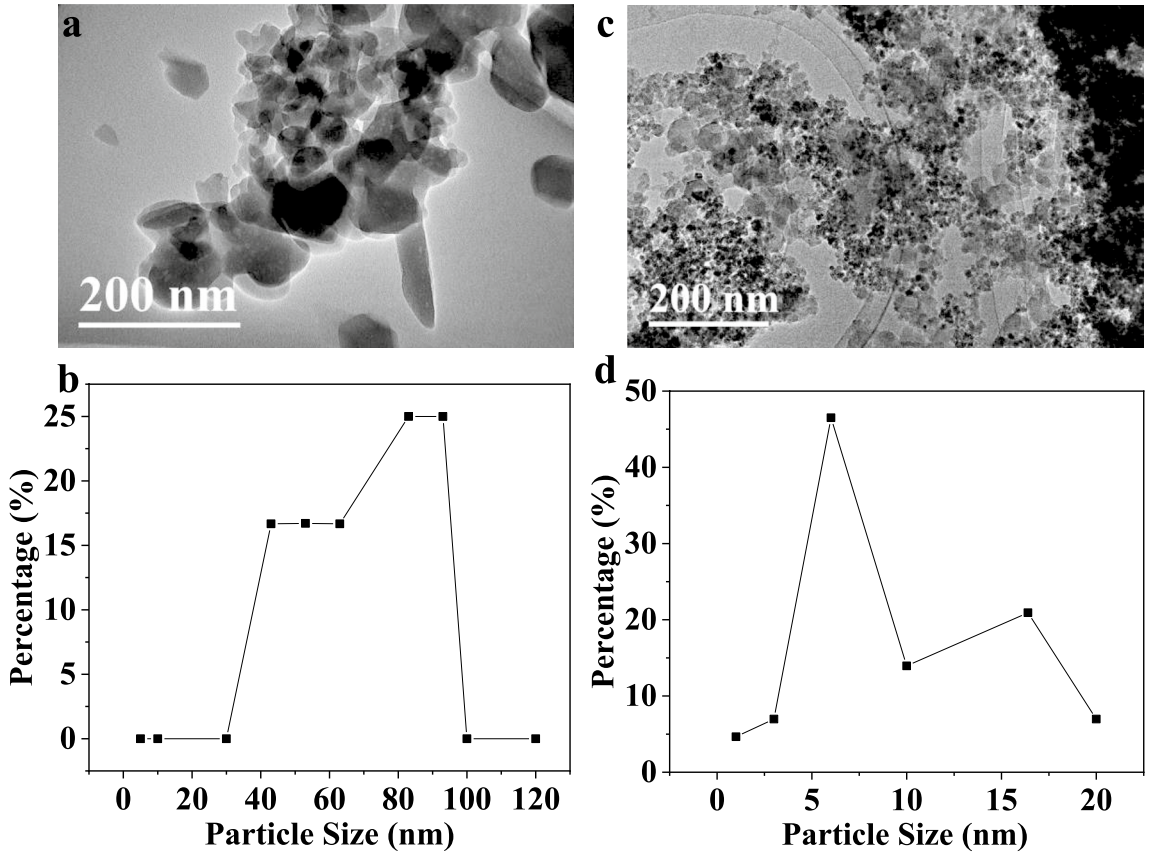

Fig. 3 **a**, **c** TEM images and **b**, **d** particle size distribution of **d** ZIF-8 and **d** MNPs for **a**–**b** ZIF-8 and **c**–**d** MNPs@ZIF-8

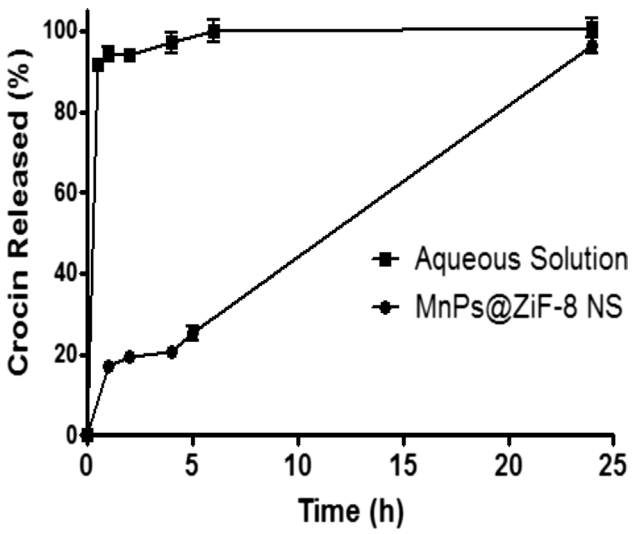

Fig. 4 The release profile of crocin from the synthesized MNPs@ZIF-8 compared to its aqueous solution

hydrophilicity. The complete release of the drug from the synthesized ZIF-8 in 24 hours confirms the surface loading of the drug rather than its encapsulation in the network pores. This profile is usually promising for cancerous cells for decreasing the times of administration of the chemotherapeutic agents [44].

As shown in Fig. 5a, increasing the concentration of the crocin-loaded MNPs@ZIF-8 offered a significant drop in the cell viability of MCF-7 compared to the crocin and the plain MNPs@ZIF-8. The IC_{50} values were 419 ± 0, 716 ± 160, and > 1000 µg/mL for the crocin-loaded MNPs@ZIF-8, crocin solution, and MNPs@ZIF-8, respectively (Fig. 5b).

Crocin was proven to interfere with the AKT/mTORC pathways that are considered key players in cell survival, proliferation, and metabolism [3]. Moreover, it was found to be involved in autophagic apoptosis [45]. Furthermore, crocin was demonstrated to inhibit the VEGFR2 gene expression in the MCF-7 cancer cell line. This expression is usually related to angiogenesis [46, 47]. The higher cytotoxic effect of the crocin-loaded MNPs@ZIF-8 can be ascribed to different causes. The MNPs@ZIF-8 can affect cell membranes and damage them with subsequent cytotoxic effects [48]. The plain ZIF-8 were previously reported to possess high cytotoxicity on MCF-7 (200 µM after 24 h incubation) [19]. Moreover, the high surface area ensures high cell contact and adhesion with the subsequent internalization of the released drug which hence poses a case of synergism on cytotoxicity. In other words,

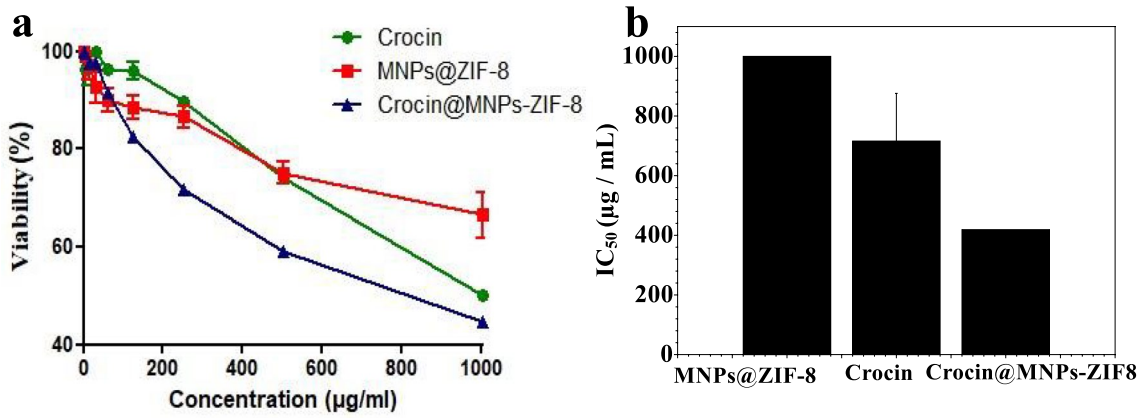

Fig. 5 **a** MCF-7 cells viability and **b** IC_{50} of materials with and without crocin. Results represent means ± SD

a carrier-obtained synergistic effect could have a role in the cytotoxicity results of the crocin-loaded nanosystems. It is also important to mention that the ZIF-8 has been proven safe and with low toxicity on normal cells.

Conclusions

This study showed a simple method for the synthesis of MNPs@ZIF-8 composite and their application for drug delivery of a natural anti-cancer agent i.e., crocin. Data analysis ensured the synthesis of a pure phase of the materials in the nanoscale range (50–100 nm). The biological analysis revealed IC_{50} values of 419, 716, and > 1000 µg/mL for the crocin-loaded MNPs@ZIF-8, crocin aqueous solution, and MNPs@ZIF-8, respectively. These results introduced MNPs@ZIF-8 as efficient nanocarriers with associated synergistic effects for the delivery of crocin.

Supplementary Information The online version contains supplementary material available at https://doi.org/10.1007/s10876-023-02526-4.

Acknowledgments Dr. Abdelhamid thanks the Science and Technology Development Fund (Project No.42886).

Author Contributions HNA: conceptualization, funding, methodology, investigation, writing – original draft, revise, conceived the original idea, writing—review and editing, supervision. DK: investigation, methodology and writing original draft. RH: conceptualization, methodology, writing—original draft, revise, writing—review and editing, supervision.

Funding Open access funding provided by The Science, Technology & Innovation Funding Authority (STDF) in cooperation with The Egyptian Knowledge Bank (EKB). Dr. Abdelhamid thanks the Science and Technology Development Fund (Project No.42886).

Data Availability The datasets generated and/or analyzed during the current study are not publicly available but are available from the corresponding author at a reasonable request.

Declarations

Competing Interests The authors declare no conflict of interest.

Ethics Approval and Consent to Participate All ethics rules were followed accordingly.

Consent for Publication All authors agree to be published.

References

1. F. I. Abdullaev (2002). *Exp. Biol. Med.* **227**, 20–25. https://doi.org/10.1177/153537020222700104.
2. J. Escribano, G.-L. Alonso, M. Coca-Prados, and J.-A. Fernández (1996). *Cancer Lett.* **100**, 23–30. https://doi.org/10.1016/0304-3835(95)04067-6.
3. D. G. Chryssanthi, F. N. Lamari, G. Iatrou, A. Pylara, N. K. Karamanos, and P. Cordopatis (2007). *Anticancer Res.* **27**, 357–62.
4. F. Abdullaev Jafarova, H. Caballero-Ortega, L. Riverón-Negrete, R. Pereda-Miranda, R. Rivera-Luna, J. Manuel-Hernández, I. Pérez-López, and J. J. Espinosa-Aguirre (2002). *Rev. Invest. Clin.* **54**, 430–436.
5. H. A. Bakshi, G. A. Quinn, M. M. Nasef, V. Mishra, A. A. A. Aljabali, M. El-Tanani, Á. Serrano-Aroca, M. Webba Da Silva, P. A. McCarron, and M. M. Tambuwala (2022). *Cells*. https://doi.org/10.3390/cells11091502.
6. T. Ochiai, H. Shimeno, K. Mishima, K. Iwasaki, M. Fujiwara, H. Tanaka, Y. Shoyama, A. Toda, R. Eyanagi, and S. Soeda (2007).

Biochim. Biophys. Acta-Gen. Subj. **1770**, 578–584. https://doi.org/10.1016/j.bbagen.2006.11.012.
7. Y.-Q. Zheng, J.-X. Liu, J.-N. Wang, and L. Xu (2007). *Brain Res.* **1138**, 86–94. https://doi.org/10.1016/j.brainres.2006.12.064.
8. M. Hashemzaei, C. Mamoulakis, K. Tsarouhas, G. Georgiadis, G. Lazopoulos, A. Tsatsakis, E. Shojaei Asrami, and R. Rezaee (2020). *Food Chem. Toxicol.* **143**, 111521. https://doi.org/10.1016/j.fct.2020.111521.
9. L. Sheng, Z. Qian, S. Zheng, and L. Xi (2006). *Eur. J. Pharmacol.* **543**, 116–122. https://doi.org/10.1016/j.ejphar.2006.05.038.
10. S. A. Siddiqui, A. Ali Redha, E. R. Snoeck, S. Singh, J. Simal-Gandara, S. A. Ibrahim, and S. M. Jafari (2022). *Molecules* **27**, 2076. https://doi.org/10.3390/molecules27072076.
11. M. Ghasemnejad-Berenji (2021). *J Food Biochem*. https://doi.org/10.1111/jfbc.13718.
12. T. Q. Pham, F. Cormier, E. Farnworth, V. H. Tong, and M.-R. Van Calsteren (2000). *J. Agric. Food Chem.* **48**, 1455–1461. https://doi.org/10.1021/jf991263j.
13. M. A. Papandreou, C. D. Kanakis, M. G. Polissiou, S. Efthimiopoulos, P. Cordopatis, M. Margarity, and F. N. Lamari (2006). *J. Agric. Food Chem.* **54**, 8762–8768. https://doi.org/10.1021/jf061932a.
14. K. Akhtari, K. Hassanzadeh, B. Fakhraei, N. Fakhraei, H. Hassanzadeh, and S. A. Zarei (2013). *Theor. Chem.* **1013**, 123–129. https://doi.org/10.1016/j.comptc.2013.03.015.
15. S. Bastani, V. Vahedian, M. Rashidi, A. Mir, S. Mirzaei, I. Alipourfard, F. Pouremamali, H. Nejabati, J. Kadkhoda, N. F. Maroufi, and M. Akbarzadeh (2022). *Biomed. Pharmacother.* **153**, 113297. https://doi.org/10.1016/j.biopha.2022.113297.
16. S. H. Alavizadeh and H. Hosseinzadeh (2014). *Food Chem. Toxicol.* **64**, 65–80. https://doi.org/10.1016/j.fct.2013.11.016.
17. R. Naderi, A. Pardakhty, M. F. Abbasi, M. Ranjbar, and M. Iranpour (2021). *Sci. Rep.* **11**, 23525. https://doi.org/10.1038/s41598-021-02073-w.
18. H. Fan, G. Fu, S. Feng, X. He, W. Cai, and Y. Wan (2023). *Food Hydrocoll.* **136**, 108279. https://doi.org/10.1016/j.foodhyd.2022.108279.
19. R. F. Mendes, F. Figueira, J. P. Leite, L. Gales, and F. A. Almeida Paz (2020). *Chem. Soc. Rev.* **49**, 9121–9153. https://doi.org/10.1039/D0CS00883D.
20. X. Wang, D. Miao, X. Liang, J. Liang, C. Zhang, J. Yang, D. Kong, C. Wang, and H. Sun (2017). *Biomater. Sci.* **5**, 658–662. https://doi.org/10.1039/C6BM00915H.
21. G. Zhao, Z. Li, B. Cheng, X. Zhuang, and T. Lin (2023). *Sep. Purif. Technol.* **315**, 123754. https://doi.org/10.1016/j.seppur.2023.123754.
22. M. Yue, Y. Fu, C. Zhang, J. Fu, S. Wang, and J. Liu (2022). *Chinese Chem. Lett.* **33**, 3291–3295. https://doi.org/10.1016/j.cclet.2021.12.015.
23. H. N. Abdelhamid (2023). *Nanosyst*. https://doi.org/10.1016/B978-0-323-85784-0.00006-6.
24. H. N. Abdelhamid, I. M. A. Mekhemer, and A.-A.M. Gaber (2023). *Mol. Catal.* **548**, 113418. https://doi.org/10.1016/j.mcat.2023.113418.
25. W. Shamroukh and H. N. Abdelhamid (2022). *J Clust Sci*. https://doi.org/10.1007/s10876-022-02402-7.
26. A. A. Sadek, M. Abd-Elkareem, H. N. Abdelhamid, S. Moustafa, and K. Hussein (2022). *BMC Vet. Res.* **18**, 260. https://doi.org/10.1186/s12917-022-03347-9.
27. H. N. Abdelhamid (2023). *Dalt Trans*. **52**, 2506–2517. https://doi.org/10.1039/D2DT04084K.
28. Q. Wang, Y. Sun, S. Li, P. Zhang, and Q. Yao (2020). *RSC Adv.* **10**, 37600–37620. https://doi.org/10.1039/D0RA07950B.
29. C. Zheng, Y. Wang, S. Z. F. Phua, W. Q. Lim, and Y. Zhao (2017). *ACS Biomater. Sci. Eng.* **3**, 2223–2229. https://doi.org/10.1021/acsbiomaterials.7b00435.
30. S. Feng, X. Zhang, D. Shi, and Z. Wang (2020). *Front Chem Sci Eng*. https://doi.org/10.1007/s11705-020-1927-8.
31. L. R. de Moura Ferraz, A. É. G. A. Tabosa, D. D. S. da Silva Nascimento, A. S. Ferreira, V. de Albuquerque Wanderley Sales, J. Y. R. Silva, S. A. Júnior, L. A. Rolim, J. J. de Souza Pereira, and P. J. Rolim-Neto (2020). *Sci. Rep.* **10**, 16815. https://doi.org/10.1038/s41598-020-73848-w.
32. S. Sanaei-Rad, M. A. Ghasemzadeh, and S. M. H. Razavian (2021). *Sci. Rep.* **11**, 18734. https://doi.org/10.1038/s41598-021-98133-2.
33. H. Nasser Abdelhamid, S. Sultan, and A. P. Mathew (2023). *Chem. Eng. J.* **468**, 143567. https://doi.org/10.1016/j.cej.2023.143567.
34. H. N. Abdelhamid, S. Sultan, and A. P. Mathew (2023). *Dalt Trans*. https://doi.org/10.1039/D2DT04168E.
35. F.E.-Z.A. Abd El-Aziz, N. E. Ebrahem, and H. N. Abdelhamid (2022). *Sci. Rep.* **12**, 14240. https://doi.org/10.1038/s41598-022-18322-5.
36. A. F. Abdel-Magied, H. N. Abdelhamid, R. M. Ashour, L. Fu, M. Dowaidar, W. Xia, and K. Forsberg (2022). *Chem Eng*. https://doi.org/10.1016/j.jece.2022.107467.
37. H. N. Abdelhamid, H. M. El-Bery, A. A. Metwally, M. Elshazly, and R. M. Hathout (2019). *Carbohydr. Polym.* **214**, 90–99. https://doi.org/10.1016/j.carbpol.2019.03.024.
38. S. M. Abdel-Hafez, R. M. Hathout, and O. A. Sammour (2018). *Colloids Surf. B Biointerfaces.* **167**, 63–72. https://doi.org/10.1016/j.colsurfb.2018.03.051.
39. E. M. El-Marakby, R. M. Hathout, I. Taha, S. Mansour, and N. D. Mortada (2017). *Int. J. Pharm.* **525**, 123–138. https://doi.org/10.1016/j.ijpharm.2017.03.081.
40. R. Yehia, R. M. Hathout, D. A. Attia, M. M. Elmazar, and N. D. Mortada (2017). *Colloids Surf. B Biointerfaces.* **155**, 512–521. https://doi.org/10.1016/j.colsurfb.2017.04.031.
41. H. Abdelrady, R. M. Hathout, R. Osman, I. Saleem, and N. D. Mortada (2019). *Eur. J. Pharm. Sci.* **133**, 115–126. https://doi.org/10.1016/j.ejps.2019.03.016.
42. S. Safwat, R. A. H. Ishak, R. M. Hathout, and N. D. Mortada (2017). *Drug Dev. Ind. Pharm.* **43**, 1112–1125. https://doi.org/10.1080/03639045.2017.1293681.
43. S. Safwat, R. M. Hathout, R. A. Ishak, and N. D. Mortada (2017). *J. Liposome Res.* **27**, 1–10. https://doi.org/10.3109/08982104.2015.1137313.
44. M. Ossama, R. M. Hathout, D. A. Attia, and N. D. Mortada (2019). *ACS Omega.* **4**, 11293–11300. https://doi.org/10.1021/acsomega.9b01580.
45. C. Yao, B.-B. Liu, X.-D. Qian, L.-Q. Li, H.-B. Cao, Q.-S. Guo, and G.-F. Zhou (2018). *Onco. Targets. Ther.* **11**, 2017–2028. https://doi.org/10.2147/OTT.S154586.
46. N. V. Fares, H. Abd-Allah, A. E. Sobaih, H. Atta, N. Ramekh, H. Khaled, M. William, J. Adel, A. Waheed, Y. Hisham, O. Mostafa, D. Sharbek, M. Samir, and R. M. Hathout (2020). *J. Drug Deliv. Sci. Technol.* **57**. https://doi.org/10.1016/j.jddst.2020.101663.
47. M. Mousavi, J. Baharara, and K. Shahrokhabadi (2014). *Avicenna J. Med. Biotechnol.* **6**, 123–127.
48. D. Plachá and J. Jampilek (2019). *Nanomaterials* **9**, 1758. https://doi.org/10.3390/nano9121758.